

Article

Microstructure and Mechanical Properties of Fiber Laser Welding of Aluminum Alloy with Beam Oscillation

Xiaobing Pang ^{1,*}, **Jiahui Dai** ², **Shun Chen** ² and **Mingjun Zhang** ² ¹ College of Mechanical & Electrical Engineering, Changsha University, Changsha 410022, China² Key Laboratory of High-Performance Intelligent Manufacturing of Mechanical Equipment of Hunan Province, Changsha University of Science & Technology, Changsha 410114, China;
djh1479334572@163.com (J.D.); cspf110702@hotmail.com (S.C.); hnuzmj@163.com (M.Z.)

* Correspondence: pangxiaobing55@ccsu.edu.cn; Tel./Fax: +86-731-8426-1492

Received: 10 October 2019; Accepted: 22 November 2019; Published: 25 November 2019



Abstract: Laser welding with beam oscillation is applied to join aluminum alloy plates in butt configuration. The effects of beam oscillating patterns on the quality of welds are compared and analyzed. The results indicate that beam oscillation can improve the weld formation and microstructure of butt joints. The circular oscillating weld has the features of fine grain and uniformly dispersed dendrites in the strengthening phase, and the porosity inhibitory effect of circular oscillation is the most obvious. In addition, beam oscillation has few effects on the tensile strength of welds, but exerts an influence on the elongation of welds.

Keywords: fiber laser welding; aluminum alloy; beam oscillation; microstructure; mechanical properties

1. Introduction

Aluminum alloys are an important engineering material in the automobile, rail, and aerospace industries as the overall performance meets the requirements of mechanical strength and low weight [1–4]. When aluminum alloy parts are used, a welding process is often needed to join the aluminum alloy parts with other components or structures. The weldability of an aluminum alloys is varied with different types of aluminum alloys. To some degree, the existence of magnesium, zinc, and silicon elements can improve the weldability of aluminum alloys due to the lower thermal conductivity and melting temperature [5]. The 5000-series aluminum alloys have better weldability than other types of aluminum alloys [5,6]. Various welding techniques are available [7–9]. In comparison with traditional welding techniques, laser beam welding has the advantages of a high energy density, a high welding speed, a deeper penetration depth, and a small heat-affected zone (HAZ) [10–15]. Therefore, this paper is especially intended to discuss a laser welding process that can meet the aforementioned requirements of a joining process.

Beam oscillation technology is proposed during electron beam welding [16], and then transplanted to laser beam welding [17,18]. Previously, laser beam oscillation was obtained by the mechanical swing of a welding head with low frequency and poor stability. However, a high-power galvanometer scanner was developed and widely used for laser beam oscillation due to its high frequency and high flexibility. Currently, laser welding with beam oscillation is applied widely in remote laser welding for its good weldability [19–22]. The primary cause of good weldability with an oscillating beam is the dilution degree of the melt pool. Therefore, laser beam oscillating welding is more popular in the industry. Zhang et al. [17] demonstrated that a good weld quality without porosity could be achieved

with a weaving laser beam during the laser welding of carbon steel. Hao et al. [23] investigated the influences of beam oscillating parameters on the weld appearance during the laser welding of austenitic stainless steel. Wang et al. [24,25] found that beam oscillation stabilized the process and improved weld morphology. Furthermore, the elongation of welds was increased. Müller et al. [26] documented that beam oscillation strategies could improve the gap bridge ability in fillet welding. Hagenlocher et al. [27] revealed that the equiaxed dendritic grain was prone to be generated without the formation of hot cracks during the laser oscillation welding of aluminum. Kraetzsch et al. [28] argued that fiber laser welding with beam oscillation offered possibilities for crack-free welding of dissimilar Al-Cu metals, comparable to the electron beam. Kim et al. [29] observed that the solidification crack disappeared at a weaving frequency of 5 Hz during laser weave welding of a self-restraint tapered aluminum alloy. Berend et al. [30] found that the humping defect of aluminum alloy welds could be suppressed by high-frequency oscillation and the welding process could be stabilized under high-speed welding.

In summary, the research on laser beam oscillating welding is still at an initial stage [31]. Studies have indicated that laser oscillation welding has the advantages of process stability and good welding quality. However, the effects of beam oscillation on the microstructure and mechanical properties of aluminum alloy welds have seldom been studied [24,32]. The present study makes an attempt to compare and analyze the effects of no oscillation, transverse oscillation and circular oscillation on the performance of aluminum alloy butt welding through a welding test on a 4-mm-thick 5056 aluminum alloy butt joint with a fiber laser and a wobble laser welding head. The weld appearance, metallurgical, and mechanical properties of the butt-welded joints are analyzed comparatively.

2. Design of Experiments

Figure 1 displays the setup of the experiments. A continuous-wave fiber laser (YLR-6000-CL; IPG Photonics Co., Oxford, MA, USA) was used as the laser source. The laser beam emitted from the end of the operation fiber was collimated and focused with a wobble laser welding head (FLW-D50-W). The laser beam emitted from the end of the optical fiber was collimated by a lens with a focal length of 200 mm and afterwards was transmitted by a galvanometer scanner unit and focused on the specimen surface by an f-theta focusing unit with a focal length of 300 mm. The spot size of the focused laser beam was approximately 0.225 mm.

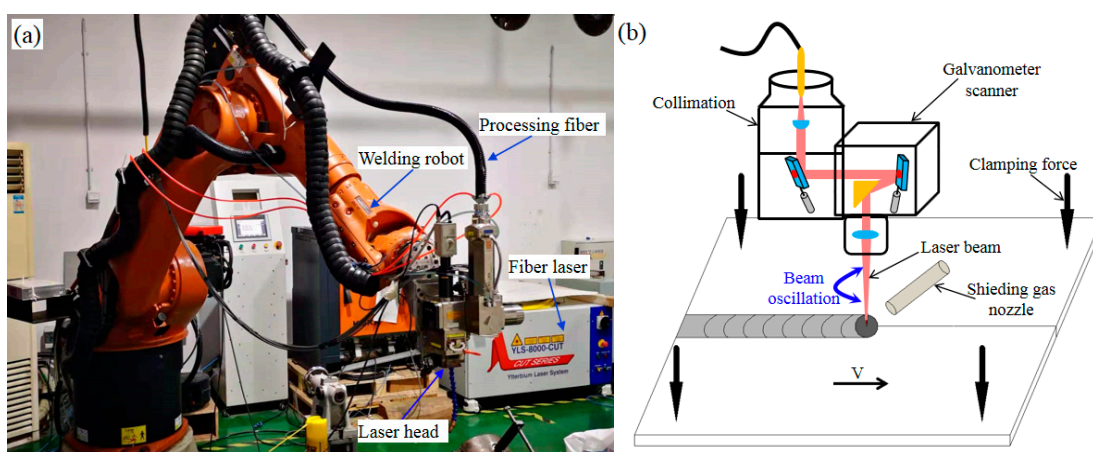


Figure 1. Experimental setup: (a) equipment and (b) schematic of laser oscillation welding process.

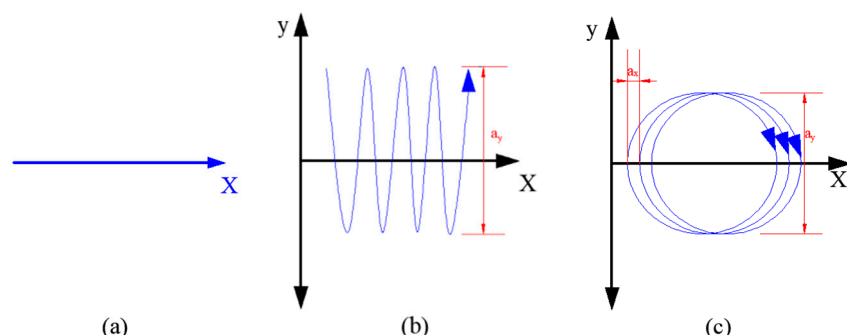
Four-millimeter-thick 5056 aluminum alloy plates were used as welding materials. Table 1 summarizes the chemical composition of the substrate. Table 2 gives the processing parameters of the laser welding experiments. Figure 2 is the schematic diagram of beam oscillating pattern. The oscillating patterns applied in our experiments are transversal and circular. The beam oscillation diameter/width a_y is 1 mm, and the value of the degree of beam overlap a_x is 0.3 mm.

Table 1. Chemical composition of the aluminum alloy studied.

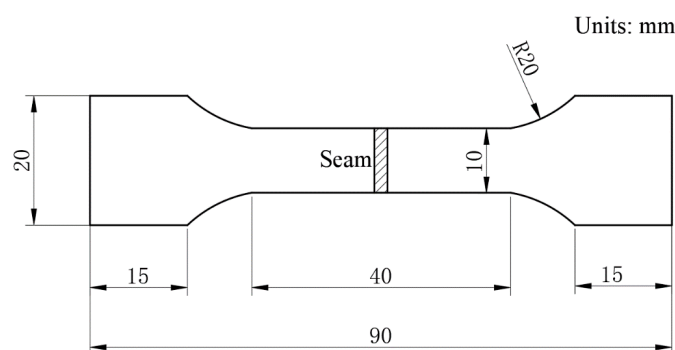
Element	Cu	Cr	Mn	Si	Mg	Zn	Fe	Al
(wt.%)	0.10	0.05	0.05	0.30	4.5	0.10	0.40	Bal.

Table 2. Parameters used in the experiments.

Weld No.	#1	#2	#3
Oscillating pattern	No	Transversal	Circle
Laser power (W)	1700	2200	2800
Oscillating frequency (Hz)	-	100	100
Welding speed (m/min)	1.8	1.8	1.8
Defocus (mm)	0	0	0
Shielding gas type	Ar	Ar	Ar
Shielding gas flow rate (L/min)	20	20	20

**Figure 2.** Schematic diagrams of beam oscillating patterns: (a) without oscillation; (b) transverse oscillation; (c) circular oscillation.

The welded plates were cut into standard tensile samples by electrodischarge machining (EDM), as illustrated in Figure 3. The cross sections of the welded joints were also cut by EDM, and then polished with abrasive paper and polishing cloth. The finished cross sections of the welded joints were etched by Keller's reagent, and then observed by an optical microscope (OM) (Leica DM4000M, Solms, Germany). The composition of the joints was tested by scanning electron microscopy (SEM) (Tescan MIRA3 LMU, Brno, Czech) equipped with an energy-dispersive X-ray spectrometer (EDS). An X-ray diffraction (XRD) instrument (Rigaku CD/max2200VPC, Tokyo, Japan) was used to identify the strengthening phase in the fusion zone of the joint. The digital and intelligent micro-hardness tester (HVST-1000Z, Ningbo, China) was used to measure the Vickers microhardness. The tester has a load of 100 g force (gf) applied in a time of 20 s. Transverse tensile tests were carried out using a universal tensile testing machine (MTS CMT5105, Eden Prairie, MN, USA) at room temperature with a crosshead speed of 1 mm/min. The fractured samples were cut and examined by SEM to reveal the fracture patterns.

**Figure 3.** Schematic illustration of transverse tensile test sample.

3. Results and Discussion

3.1. Weld Appearance

Figure 4 shows the macroscopic morphologies of the butt-welded joints. As seen in Figure 4, the formation of the top and root surfaces of the weld can be affected by beam oscillation. Specifically, the top and root surfaces of the weld are discontinuous, unsMOOTH, and narrow in width without oscillation. For the weld formed by transverse oscillation, the top and root surfaces turn out to be smoother and still have a narrow width. However, the circular oscillating weld shows great improvement in the smoothness and consistency of its top and root surfaces and has a wider width. In addition, the specimens are completely welded in any case, but, as shown in Figure 4, root sagging or undercut is obvious on the top and root surfaces of the weld without oscillation, but insignificant root sagging or undercut is noted under transverse oscillation, and less or no root sagging or undercut is observed in circular oscillation.

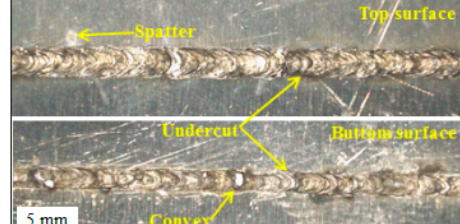
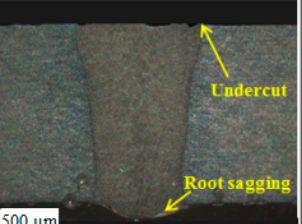
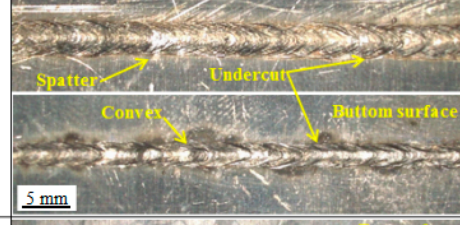
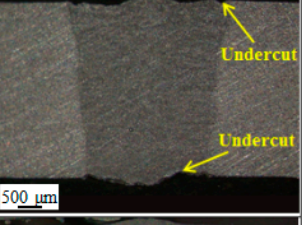
Oscillation pattern	Surface appearance (Welding direction from right to left)	Cross section
Without oscillation	 <p>Spatter Top surface Undercut Bottom surface Convex 5 mm</p>	 <p>Undercut Root sagging 500 μm</p>
Transverse oscillation	 <p>Spatter Top surface Undercut Bottom surface Convex 5 mm</p>	 <p>Undercut Undercut 500 μm</p>
Circular oscillation	 <p>Spatter Top surface Bottom surface 5 mm</p>	 <p>500 μm</p>

Figure 4. Surface appearances and cross section morphologies of welded joints at oscillation pattern.

3.2. Microstructure

Figure 5 demonstrates the optical micrographs of the butt joints. It is shown in Figure 5a that, in the fusion zone without oscillation, Mg_3Al_2 dendrites in the strengthening phase are accumulated and distributed inconsistently. The XRD analysis suggests that the Mg_3Al_2 phase is generated in the fusion zone of the welds, as shown in Figure 6. This can be explained by the fast cooling rate and the high degree of supercooling during the laser welding process. In contrast, Mg_3Al_2 dendrites tend to disperse in the fusion zone using transverse oscillation, as shown in Figure 5b. This is because there is a strong stirring effect in the welded keyhole, which forces the dendritic growth to disperse [32]. The fusion zone with circular oscillation is the best for the dispersion of Mg_3Al_2 dendrites, being very uniform and almost equal to that of the base material, as illustrated in Figure 5c. Therefore, we can conclude that the microstructure of the weld is significantly improved and the mechanical properties seem to be better with beam oscillation. As seen in Figure 5d, the grains at the heat-affected zone of the welds with beam oscillation grow to equiaxed dendrites more easily without columnar

dendrites, which generally appear in laser welding without beam oscillation. This can be attributed to the periodic cycles of keyhole expansion and shrinkage in laser welding with beam oscillation [32].

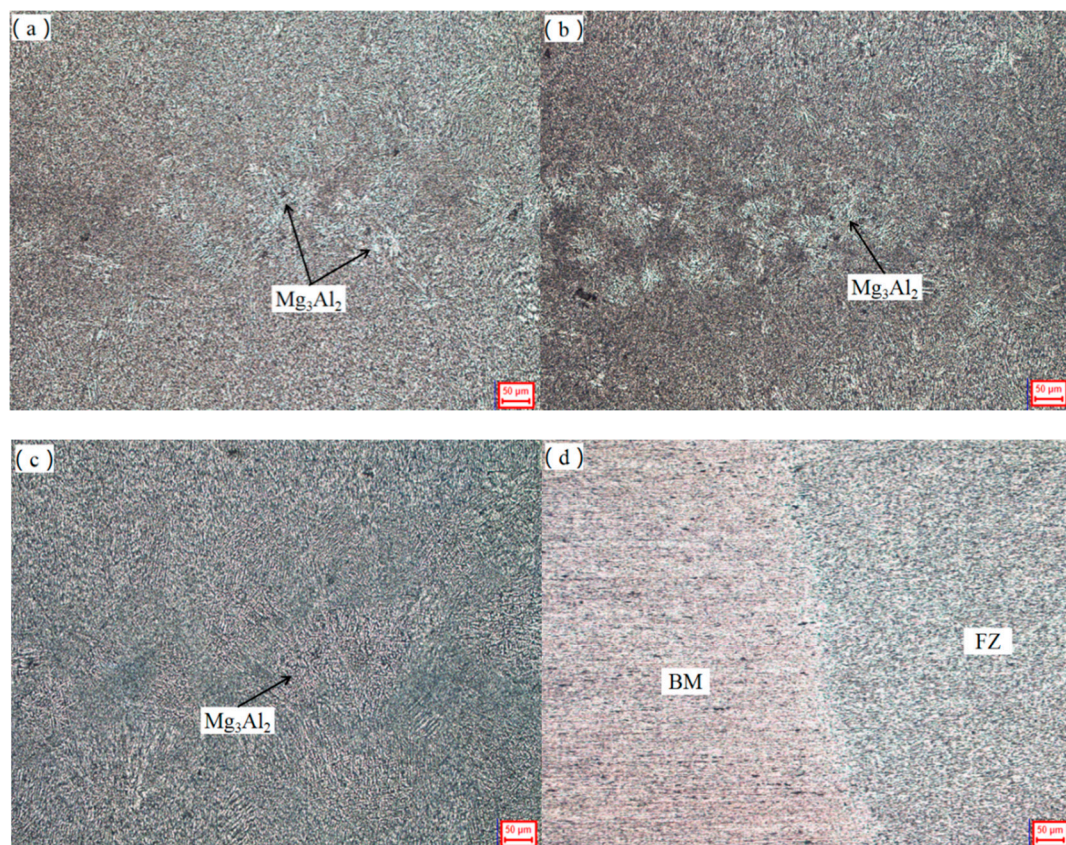


Figure 5. Microstructures of butt joints: (a) fusion zone without oscillation; (b) fusion zone with transverse oscillation; (c) fusion zone with circular oscillation; (d) heat-affected zone with circular oscillation.

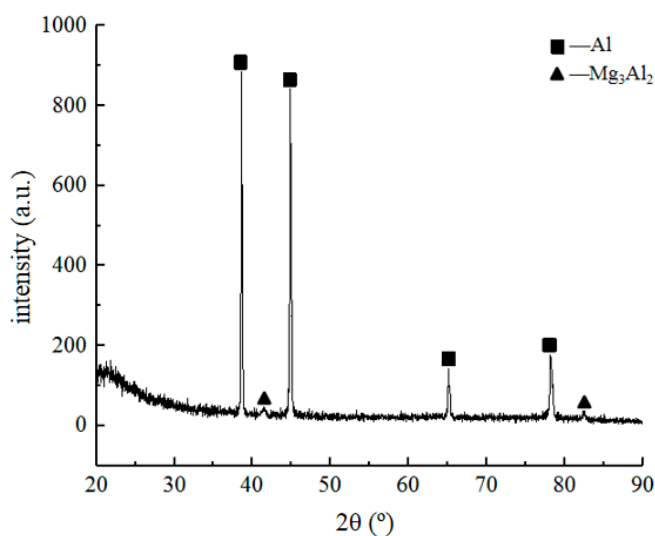


Figure 6. X-ray diffraction profile of the joint welded with transverse oscillation.

3.3. Mechanical Properties

Figure 7 is the cross-sectional hardness distribution of welds in different beam oscillation modes. The averages of three measurements is shown as one point in Figure 7. It is determined from Figure 7

that no significant difference is identified between the hardness of welds in the three beam oscillation modes, and also no difference between the hardness in different regions' base material (BM), fusion zone (FZ), and heat-affected zone (HAZ). In particular, the average microhardness of the fusion zone of the circular oscillating weld is max. 69.50 HV vs. min. 68.71 HV, compared to the weld without oscillation. Moreover, the change in microhardness change in the fusion zone of the weld is greater with oscillation than with circular or transverse oscillation. This confirms that beam oscillation has a beneficial effect on the uniform distribution of the fusion zone microstructure. In addition, the microhardness value of the annealed base material before welding is 66.83 HV. In summary, the microhardness of the weld is well matched to the metallographic microstructure, and the hardness of the weld and the heat-affected zone are both higher than those of the base material. An explanation for this is that the heat input is concentrated, the heating and cooling times are extremely short, and the weld structure formed is very small during laser welding, thus increasing the hardness. In other words, the circular oscillating weld has the finest and most dispersed dendrites and thus the largest microhardness, which confirms the Hall-Petch relationship.

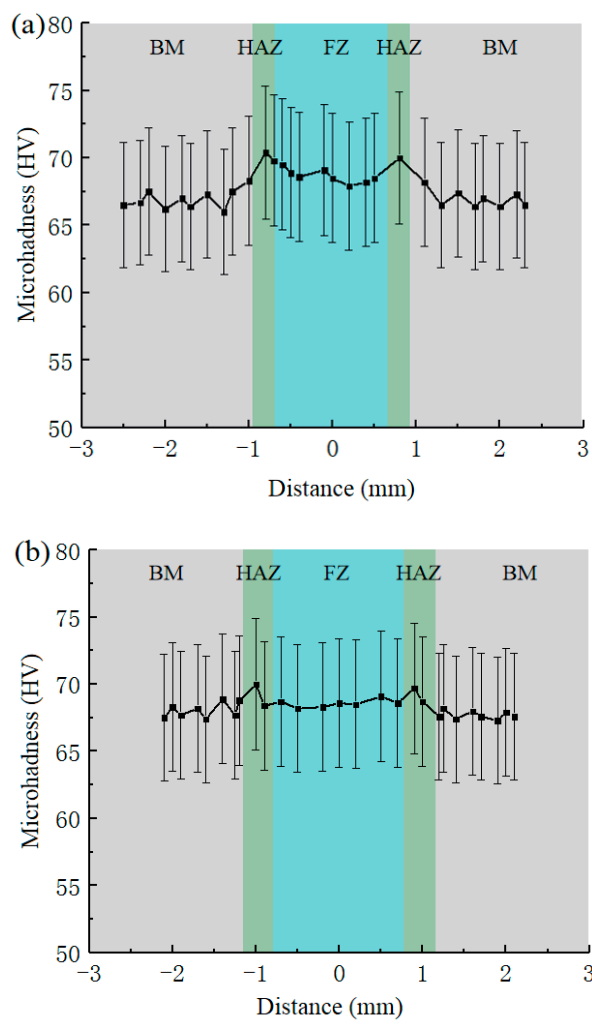


Figure 7. Cont.

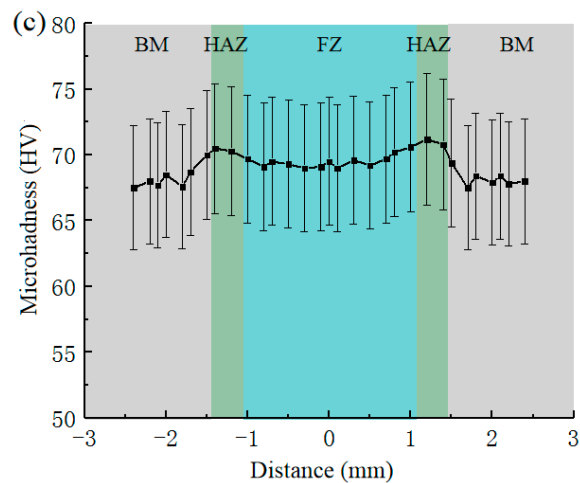


Figure 7. Microhardness profiles of butt joints: (a) without oscillation; (b) transverse oscillation; (c) circular oscillation.

The transverse tensile test represents an effort to assess the tensile strength of the butt joints. The stress-strain curves of welds are displayed in Figure 8. The tensile strength of joints welded with or without beam oscillation is 212–215 MPa, which lends support to the idea that the beam oscillation and weld surface conditions exert only minor influences on the weld tensile strength. However, the beam oscillation is an important predictor of weld ductility. The circular oscillating weld has the biggest strain of about 6.0%, 17.6% higher than that of the weld without oscillation (5.1%). The elongation of a transversely oscillating weld is measured at about 5.8%. According to [24], this is due to the increased proportion of equiaxed grains in the weld under circular oscillation.

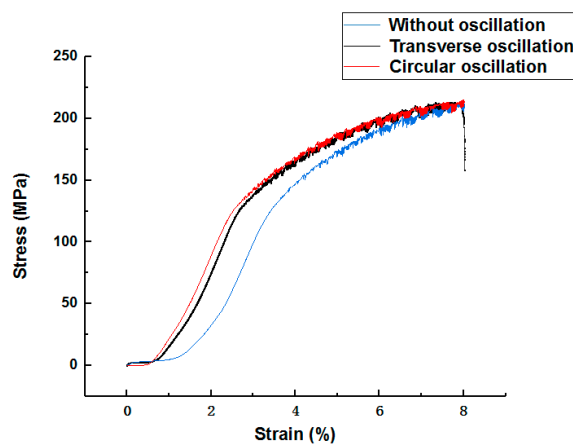


Figure 8. Stress-strain curves of the welded specimens.

Figure 9 is a graph showing the fracture effect of a tensile specimen. As indicated in Figure 9a,d, the specimen without oscillation starts to fracture from the undercut, and ends at the weld fusion zone after tension. A large pore is seen in the fracture, the presence of which reduces the force area and thus increases the tensile strength of the weld. The cause of the pores in the welds is the instability of the keyhole [33]. Porosity is a typical effect during the laser welding of aluminum. A similar fracture pattern is established after tension in a specimen welded with transverse oscillation, compared to one without oscillation, as shown in Figure 9b. However, for the circular oscillating specimen, the fracture starts from the heat-affected zone of the weld, and ends at the weld fusion zone, as indicated in Figure 9c. In addition, no obvious pore is observed in the fractures of the welds with transverse oscillation and circular oscillation, as evidenced in Figure 9e,f. This sheds light on the fact that the undercut defect of the surface weld is a weak part of the welded joint, and can be improved by the

application of circular oscillation. It should be noted that all the fractures of the specimen are 45° from the direction of the tensile stress applied, which is the ductile shear fracture [27].

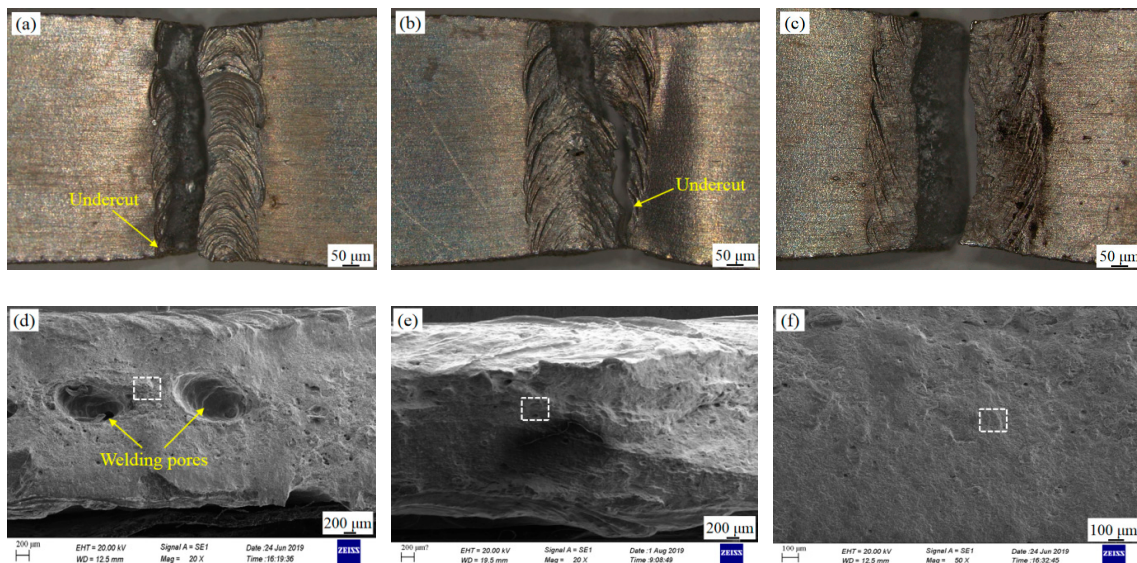


Figure 9. Macroscopic views of the fractured tensile specimens: (a) and (d) without oscillation; (b) and (e) transverse oscillation; (c) and (f) circular oscillation.

In order to explore the causes of the variation of tensile strength and plasticity of butt joints, the fracture surfaces of the tensile samples were observed by SEM, as shown in Figure 10. The morphology of the joint welded without beam oscillation exhibited a fracture with characteristic pores and dimples, as shown in Figure 9d and 10a. This indicated that the test specimen failed as a ductile fracture with the feature of dimple/microvoid coalescence. The pores worsened the stress concentration in the weld during tensile testing, and resulted in the reduced tensile strength and toughness of the weld. The transversely oscillating specimen also showed a ductile fracture, which conforms a dimple/microvoid coalescence pattern in which the fracture has many dimples but few pores, as displayed in Figure 10b,c. In the circularly oscillating specimen, numerous cavities were seen on the fractured blade, as shown in Figure 9f. This was ascribed to the vast reinforced phase particles that were pulled out from the weld bead during tensile testing. It is evident that the appearance of reinforced phase particles led to the higher dispersion strengthening of the weld bead. The formation of dense small dimples with a higher depth-diameter ratio confirmed the hypothesis that the plasticity of a joint welded with circular oscillation was good, which was consistent with the tensile stress-stain curve and the macroscopic necking phenomenon of the tensile samples.

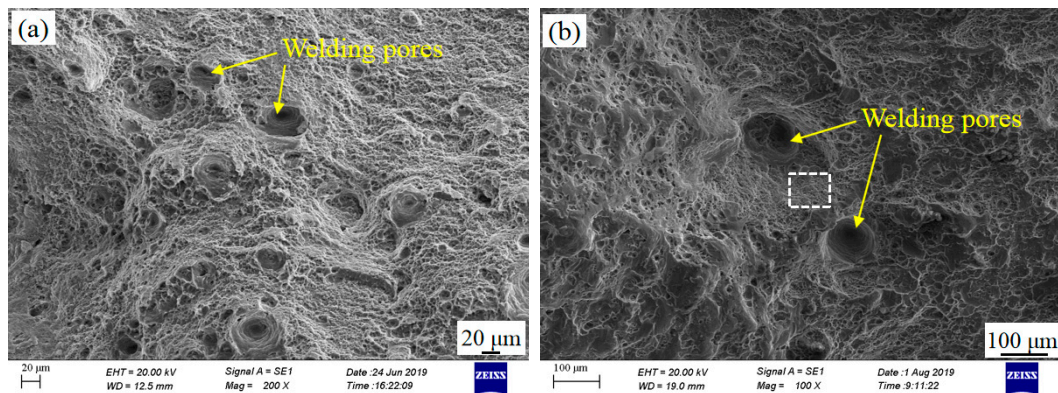


Figure 10. Cont.

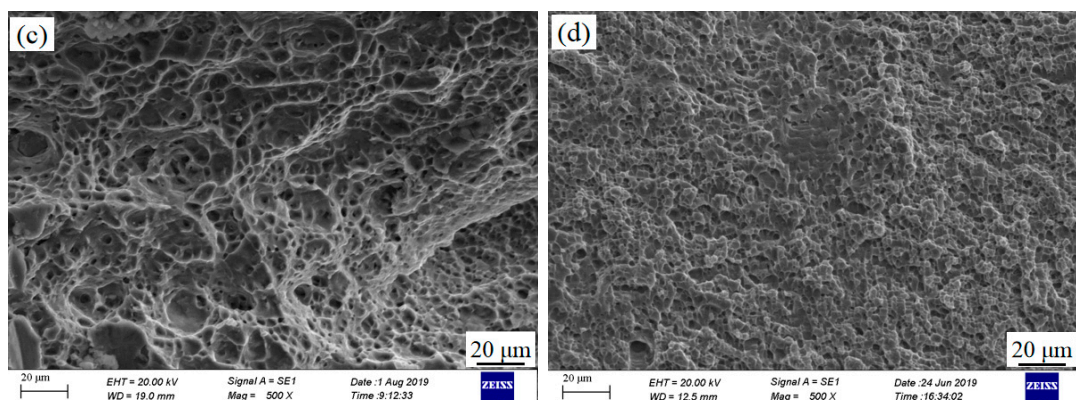


Figure 10. SEM morphologies of the fractured surfaces: (a) without oscillation; (b) transverse oscillation; (c) magnified image of the zone inside the dotted rectangle in (b); (d) circular oscillation.

4. Conclusions

Motivated by the scarcity of research on the welded joint of a fiber laser welding aluminum alloy with beam oscillation, we conducted a laser welding experiment on 5056 aluminum alloy specimens, and analyzed the appearance, microstructure, hardness, and strength properties of welded joints. The following conclusions were made after the experiment.

- (1) Beam oscillation causes great improvements in the weld formation of laser butt welding of aluminum alloy. The surface of the weld with circular oscillation is well formed and has good consistency without spatter, undercut, and root sagging.
- (2) Beam oscillation results in a significant improvement of the weld microstructure of laser butt welding of aluminum alloy. The circular oscillating weld has the features of fine grain and uniformly dispersed dendrites in the strengthening phase, and the largest microhardness is observed in the fusion zone.
- (3) Beam oscillation is significantly inhibitory to the porosity of the weld, and the inhibitory effect is even stronger with circular oscillation than with transverse oscillation. There is no pore in the tensile fracture of the circular oscillating weld, but a small number of pores can be seen in the corresponding position of a transversely oscillating weld, and many more pores with a large volume are noted without oscillation. Beam oscillation has few effects on the tensile strength of the weld, but exerts a great influence on the elongation of the weld, which is evidenced by the fact that the largest elongation of the weld is associated with circular oscillation.

Author Contributions: Conceptualization, M.Z.; Funding acquisition, M.Z.; Investigation, X.P. and J.D.; Methodology, S.C.; Supervision, S.C.; Writing—original draft, X.P. and J.D.; Writing—review & editing, M.Z.

Funding: This research was funded by the National Natural Science Foundation of China grant number [51605045] and the Natural Science Foundation of Hunan Province of China grant number [2018JJ2437].

Conflicts of Interest: The authors declare no conflicts of interest.

References

1. Tan, C.; Yang, J.; Zhao, X.; Zhang, K.; Song, X.; Chen, B.; Feng, J. Influence of Ni coating on interfacial reactions and mechanical properties in laser welding-brazing of Mg/Ti butt joint. *J. Alloy. Compd.* **2018**, *764*, 186–201. [[CrossRef](#)]
2. Zhou, L.; Li, G.H.; Zhang, R.X.; Zhou, W.L.; He, W.X.; Huang, Y.X.; Song, X.G. Microstructure evolution and mechanical properties of friction stir spot welded dissimilar aluminum-copper joint. *J. Alloy. Compd.* **2019**, *775*, 372–382. [[CrossRef](#)]
3. Geng, H.; Xia, Z.; Zhang, X.; Li, G.; Cui, J. Microstructures and mechanical properties of the welded AA5182/HC340LA joint by magnetic pulse welding. *Mater. Charact.* **2018**, *138*, 229–237. [[CrossRef](#)]

4. Chen, S.; Yang, D.; Li, M.; Zhang, Y.; Huang, J.; Yang, J.; Zhao, X. Laser penetration welding of an overlap titanium-on-aluminum configuration. *Int. J. Adv. Manuf. Technol.* **2016**, *87*, 3069–3079. [[CrossRef](#)]
5. Sánchez-Amaya, J.M.; Boukha, Z.; Amaya-Vázquez, M.R.; Botana, F.J. Weldability of aluminum alloys with high-power diode laser. *Weld. J.* **2012**, *91*, 155–161.
6. Mossman, M.M.; Lippold, J.C. Weldability testing of dissimilar combinations of 5000-and 6000-series aluminum alloys. *Weld. J.* **2002**, *81*, 188–194.
7. Xue, J.; Xu, M.; Huang, W.; Zhang, Z.; Wu, W.; Jin, L. Stability and Heat Input Controllability of Two Different Modulations for Double-Pulse MIG Welding. *Appl. Sci.* **2019**, *9*, 127. [[CrossRef](#)]
8. Li, H.; Gao, J.; Li, Q. Fatigue of Friction Stir Welded Aluminum Alloy Joints: A Review. *Appl. Sci.* **2018**, *8*, 2626. [[CrossRef](#)]
9. Jo, H.; Kim, D.; Kang, M.; Park, J.; Kim, Y.M. Effects of Surface Roughness and Force of Electrode on Resistance Spot Weldability of Aluminum 6061 Alloy. *Appl. Sci.* **2019**, *9*, 3958. [[CrossRef](#)]
10. Zhang, M.; Chen, S.; Zhang, Y.; Chen, G.; Bi, Z. Mechanisms for Improvement of Weld Appearance in Autogenous Fiber Laser Welding of Thick Stainless Steels. *Metals* **2018**, *8*, 625. [[CrossRef](#)]
11. Zou, J.L.; Wu, S.K.; Yang, W.X.; He, Y.; Xiao, R.S. A novel method for observing the micro-morphology of keyhole wall during high-power fiber laser welding. *Mater. Des.* **2016**, *89*, 785–790. [[CrossRef](#)]
12. Mei, L.; Yan, D.; Chen, G.; Xie, D.; Zhang, M.; Ge, X. Comparative study on CO₂ laser overlap welding and resistance spot welding for automotive body in white. *Mater. Des.* **2015**, *78*, 107–117. [[CrossRef](#)]
13. Zhang, L.J.; Zhang, G.F.; Ning, J.; Zhang, X.J.; Zhang, J.X. Microstructure and properties of the laser butt welded 1.5-mm thick T2 copper joint achieved at high welding speed. *Mater. Des.* **2015**, *88*, 720–736. [[CrossRef](#)]
14. Sofia, D.; Barletta, D.; Poletto, M. Laser sintering process of ceramic powders: The effect of particle size on the mechanical properties of sintered layers. *Addit. Manuf.* **2018**, *23*, 215–224. [[CrossRef](#)]
15. Sofia, D.; Granece, M.; Barletta, D.; Poletto, M. Laser sintering of unimodal distributed glass powders of different size. *Proced. Eng.* **2015**, *102*, 749–758. [[CrossRef](#)]
16. Sun, Z.; Karppi, R. The application of electron beam welding for the joining of dissimilar metals: An overview. *J. Mater. Process. Technol.* **1996**, *59*, 257–267. [[CrossRef](#)]
17. Zhang, X.D.; Chen, W.Z.; Bao, G.; Zhao, L. Improvement of weld quality using a weaving beam in laser welding. *J. Mater. Sci. Technol.* **2004**, *20*, 633–636.
18. Hao, K.; Gao, M.; Wu, R.; Zeng, X. Effect of oscillating laser beam offset on the microstructure and mechanical properties of dissimilar stainless steels joints. *J. Mater. Process. Technol.* **2020**, *275*, 116330. [[CrossRef](#)]
19. Sommer, M.; Webergals, J.P.; Müller, S.; Berger, P.; Graf, T. Advantages of laser beam oscillation for remote welding of aluminum closely above the deep-penetration welding threshold. *J. Laser Appl.* **2017**, *29*, 012001. [[CrossRef](#)]
20. Fetzer, F.; Sommer, M.; Weber, R.; Webergals, J.P.; Graf, T. Reduction of pores by means of laser beam oscillation during remote welding of AlMgSi. *Opt. Lasers Eng.* **2018**, *108*, 68–77. [[CrossRef](#)]
21. Schweier, M.; Haubold, M.W.; Zaeh, M.F. Analysis of spatters in laser welding with beam oscillation: A machine vision approach. *CIRP J. Manuf. Sci. Technol.* **2016**, *14*, 35–42. [[CrossRef](#)]
22. Haubold, M.W.; Zäh, M.F. Real-time spatter detection in laser welding with beam oscillation. *Proced. CIRP* **2019**, *79*, 159–164. [[CrossRef](#)]
23. Hao, K.; Li, G.; Gao, M.; Zeng, X. Weld formation mechanism of fiber laser oscillating welding of austenitic stainless steel. *J. Mater. Process. Technol.* **2015**, *225*, 77–83. [[CrossRef](#)]
24. Wang, L.; Gao, M.; Zhang, C.; Zeng, X. Effect of beam oscillating pattern on weld characterization of laser welding of AA6061-T6 aluminum alloy. *Mater. Des.* **2016**, *108*, 707–717. [[CrossRef](#)]
25. Wang, L.; Gao, M.; Zeng, X. Experiment and prediction of weld morphology for laser oscillating welding of AA6061 aluminium alloy. *Sci. Technol. Weld. Join.* **2019**, *24*, 334–341. [[CrossRef](#)]
26. Müller, A.; Goecke, S.F.; Rethmeier, M. Laser beam oscillation welding for automotive applications. *Weld. World* **2018**, *62*, 1039–1047. [[CrossRef](#)]
27. Hagenlocher, C.; Sommer, M.; Fetzer, F.; Weber, R.; Graf, T. Optimization of the solidification conditions by means of beam oscillation during laser beam welding of aluminum. *Mater. Des.* **2018**, *160*, 1178–1185. [[CrossRef](#)]

28. Kraetzsch, M.; Standfuss, J.; Klotzbach, A.; Kaspar, J.; Brenner, B.; Beyer, E. Laser beam welding with high-frequency beam oscillation: Welding of dissimilar materials with brilliant fiber lasers. *Phys. Proced.* **2011**, *12*, 142–149. [[CrossRef](#)]
29. Kim, C.; Kang, M.; Kang, N. Solidification crack and morphology for laser weave welding of Al 5J32 alloy. *Sci. Technol. Weld. Join.* **2013**, *18*, 57–61. [[CrossRef](#)]
30. Berend, O.; Haferkamp, H.; Meier, O.; Engelbrecht, L. High-frequency beam oscillating to increase the process stability during laser welding with high melt pool dynamics. In Proceedings of the 24th International Congress on Applications of Laser Electro-Optics, Miami, FL, USA, 31 October–3 November 2005; pp. 1032–1041.
31. Jarwitz, M.; Fetzer, F.; Weber, R.; Graf, T. Weld Seam Geometry and Electrical Resistance of Laser-Welded, Aluminum-Copper Dissimilar Joints Produced with Spatial Beam Oscillation. *Metals* **2018**, *8*, 510. [[CrossRef](#)]
32. Wang, Z.; Oliveira, J.P.; Zeng, Z.; Bu, X.; Peng, B.; Shao, X. Laser beam oscillating welding of 5A06 aluminum alloys: Microstructure, porosity and mechanical properties. *Opt. Laser Technol.* **2019**, *111*, 58–65. [[CrossRef](#)]
33. Matsunawa, A.; Mizutani, M.; Katayama, S.; Seto, N. Porosity formation mechanism and its prevention in laser welding. *Weld. Int.* **2003**, *17*, 431–437. [[CrossRef](#)]



© 2019 by the authors. Licensee MDPI, Basel, Switzerland. This article is an open access article distributed under the terms and conditions of the Creative Commons Attribution (CC BY) license (<http://creativecommons.org/licenses/by/4.0/>).